Living Poly(α-methylstyrene) near the Polymerization Line. 3. Small-Angle Neutron Scattering

A. Ploplis Andrews,† K. P. Andrews, and S. C. Greer*

Department of Chemistry and Biochemistry, The University of Maryland at College Park, College Park, Maryland 20742

F. Boué and P. Pfeuty

Laboratoire Léon Brillouin, Centre d'Études Nucleaires de Saclay, 91191 Gif-sur-Yvette Cedex, France

Received January 4, 1994; Revised Manuscript Received April 15, 1994®

ABSTRACT: We present small-angle neutron scattering measurements on the system living poly(α-methylstyrene) in deuterated tetrahydrofuran, using sodium naphthalide as the initiator. We study three samples, differing in the ratio, r, of the number of moles of initiator to the number of moles of initial monomer and differing in the mole fraction of initial monomer. We compare the data to a theory for the scattering which treats the polymerization as a phase transition in the mean field approximation and also to a theory based on the dilute $n \to 0$ magnet model (where n is the dimension of the order parameter) in which no mean field assumption is made but in which an assumption of no solvent interaction is made [Wheeler, J. C.; Pfeuty, P. M. *Phys. Rev. Lett.* **1993**, *71*, 1653]. We compare the measured concentration structure function, $S(q,T)$ (where q is the wavenumber and T is the temperature) and $S(0,T)$, the extrapolation to $q = 0$, to the theoretical predictions. We find that both the mean field theory and the dilute $n \to 0$ magnet model are able to account qualitatively for the general features of the scattering data. However, the mean field theory does not predict the maximum observed in $S(0,T)$ at temperatures below the polymerization temperature. The maximum in $S(0,T)$ is predicted by the dilute $n \to 0$ model in its zero solvent interaction limit. We determine also the characteristic length, $\xi(T)$, which increases as the living polymers form and grow, reaches a maximum at the temperature at which overlap begins, and then decreases as the polymer mesh develops. Both the mean field theory and the dilute $n \to 0$ model are in qualitative, but not quantitative, agreement with the measurements of $\xi(T)$.

I. Introduction

"Living" polymers—polymers for which the reactive ends of the molecules remain unterminated[1-3]—offer interesting phenomena for study. First, one can view the onset of polymerization at the ceiling temperature, T_p, as a phase transition and treat it either with a classical mean field theory[4,5] or with the $n \to 0$ limit of the n-vector model of a magnetic phase transition.[6,7] The application of such theories to the prediction of thermodynamic and transport properties of living polymer solutions is an object of active investigation.[8-10] Second, since below T_p the average molecular weight of a living polymer system increases as the temperature is decreased, one can vary the average molecular weight simply by changing the temperature, and then one can conveniently vary and study the nature and structure of the living polymer solution. Small-angle neutron scattering (SANS) is an especially appropriate tool for studying living polymer solutions. The scattering intensity at zero angle is a measure of the concentration susceptibility, and the scattering intensity as a function of angle reveals much about the microscopic structure of the living polymer solution. SANS does not present the problems of absorption by the colored solution, scattering by dust in the solution, and radiation-induced reactions of the living polymer which would be encountered in light scattering from these solutions.

The impediment to working with solutions of living polymers has been the difficulty of preparing samples which will remain unterminated for long periods of time. We have learned how to make samples which are essentially stable.[8-14] We have presented[15] preliminary SANS measurements on samples of living poly(α-methylstyrene) in deuterated tetrahydrofuran, using sodium naphthalide as the initiator[16] and compared the experimental data on the intensity of scattering at zero scattering angle to a mean field theory for the scattering intensity of a living polymer solution as a function of temperature.

We present here much more extensive SANS measurements on the same system: living poly(α-methylstyrene) in deuterated tetrahydrofuran, using sodium naphthalide as the initiator. We note that tetrahydrofuran is a good solvent for poly(α-methylstyrene), with a Flory interaction parameter[17,18] $\chi \sim 0.4$; we assume that the value of χ is nearly the same for living poly(α-methylstyrene) in tetradeuteriofuran. We study three samples, differing in the ratio, r, of the number of moles of initiator to the number of moles of initial monomer and differing in the mole fraction of initial monomer. We compare our measurements to two theoretical models: (1) a mean field model and (2) a non-mean field model, the dilute $n \to 0$ magnet model, where n is the dimension of the order parameter and "dilute" refers to the allowance of the model for the presence of solvent.[7] The application of the dilute $n \to 0$ model to these experiments is made possible by a recent development by Wheeler and Pfeuty[19] in which the assumption of no interaction between the monomer and the solvent permits a calculation without making a mean field assumption. We compare the measured concentration structure function, $S(q,T)$ (where q is the wavenumber and T is the temperature), and $S(0,T)$, the extrapolation to $q = 0$, to the theoretical predictions. We find that the mean field theory is able to account for the general features of the scattering data but does not predict the maximum observed in $S(0,T)$ for temperatures below T_p. The dilute $n \to 0$ model in the approximation of no solvent interaction

* To whom correspondence should be addressed.
† Present address: Department of Physics, The College of Wooster, Wooster, OH 44691.
® Abstract published in *Advance ACS Abstracts*, May 15, 1994.

0024-9297/94/2227-3902$04.50/0

does predict the maximum in $S(0,T)$. We also determine the characteristic length, $\xi(T)$, which increases as the living polymers form and grow, reaches a maximum at the temperature at which overlap begins, and then decreases as the polymer mesh develops. Both the mean field theory and the dilute $n \rightarrow 0$ model can describe qualitatively (but not quantitatively) the measured behavior of $\xi(T)$.

II. Theory

In 1980, the limit $n \rightarrow 0$ (where n is the dimension of the order parameter) of a dilute n-vector model of magnetism in a small external magnetic field was introduced to describe equilibrium polymerization in a solvent, with applications to sulfur solutions[20] and to living polymer solutions.[7] This view of equilibrium polymerization as a "magnetic" phase transition followed from the treatment of polymer solutions in the language of magnetic critical phenomena by de Gennes[21] and by des Cloizeaux.[22]

The neutron scattering experiments reported here have stimulated an extension of the dilute $n \rightarrow 0$ magnet theory to the study of the concentration structure function, $S(q,T)$, directly related to the neutron scattering intensity, $I(q,T)$, where q is the wavenumber and T is the temperature. We first consider the model in the mean field approximation, which corresponds to the Flory–Huggins theory of polymer solutions.[17] We use the $n \rightarrow 0$ magnet formalism, rather than the Flory–Huggins formalism, because the $n \rightarrow 0$ magnet model can be extended beyond the mean field approximation. We then proceed to such an extension, as recently developed by Wheeler and Pfeuty.[19]

A. Concentration Structure Function, $S(q,T)$, in the Mean Field Approximation. We start from the dilute n-vector lattice model[23] of magnetism in a small magnetic field, h, and in the limit $n \rightarrow 0$, with Hamiltonian H (eq 2.5 of ref 20b). Following the method of Furman and Blume,[24] we calculate the concentration structure function, $S(q) = \langle \nu(q)\ \nu(-q) \rangle_H$, by applying the fluctuation–dissipation principle; this corresponds to the well-known random phase approximation (RPA).[25] Here ν is the spin variable at position r on the lattice of N total sites, and $\nu(q) = (1/N)\sum \exp(iqr_n)\nu(r_n)$, where the sum is from $n = 1$ to N and $\nu(r_n)$ is 1 for a monomer and 0 for solvent. We add to H an oscillating chemical potential to get the new Hamiltonian, H':

$$H' = H - \mu \sum \exp(iqr_n)\nu(r_n) \tag{1}$$

where the sum is again for n from 1 to N, from which we find

$$(\partial \langle \nu(q) \rangle_{H'}/\partial \mu)_{\mu=0} = \langle \nu(q)\ \nu(-q) \rangle_H - \langle \nu(q) \rangle_H^2 \tag{2}$$

The first term on the right-hand side of eq 2 is $S(q)$. The left-hand side is obtained from the linearization in μ of a mean field calculation[24] of the average $\langle \nu(q) \rangle_{H'}$. After rearrangement, we get the final result in terms of initial mole fraction of monomer, x_m^*, and of the "magnetic quantities"[7,20] h (the external magnetic field), m (the magnetism), J (the spin–spin coupling), and K (a mixing energy):

$$S^{-1}(q,T) = -K(q) + [x_m^*(1 - x_m^*)]^{-1}\,[J(q)(J(0)m + h)^3]/ [(1 + {}^1/_2(J(0)m + h)^2)\,((J(0)m + {}^1/_2h)(J(0)m + h)^2 + h + m(J(0) - J(q))(1 - {}^1/_2(J(0)m + h)^2))] \tag{3}$$

The functions $J(q) = J(0)\,f(q)$ and $K(q) = K(0)\,f(q)$ result from the use of the Green's function representation.[26] The function $f(q) = (1/z)\sum \exp(iqr_n)$, where the sum is from $n = 1$ to z, depends on the lattice, the terms in the sum corresponding to the z nearest neighbors with coordinates r_n on a three-dimensional lattice. For a simple cubic lattice,[27] $f(q) = (1/3)[\cos(q_x a) + \cos(q_y a) + \cos(q_z a)]$, where "$a$" is the size of a monomer molecule, which determines the lattice parameter. For a body-centered cubic lattice,[28] $f(q) = [\cos(q_x a') \cos(q_y a') \cos(q_z a')]$, and "$a$" is $a/3^{1/2}$. For a face-centered cubic lattice, $f(q) = (1/3)[\cos(q_x a'') \cos(q_y a'') + \cos(q_x a'') \cos(q_z a'') + \cos(q_y a'') \cos(q_z a'')]$ and, "a" is $a/2^{1/2}$. For small q, we can expand $f(q)$ and get for all three lattices $f(q) \sim 1 - aq^2/6$, where "a" is the same "a" as above and $f(0) = 1$.

The quantity $J(0)$ can be identified[7,20] as $J(0) = K_p(T) = \exp(-\Delta H_p^0 + T\Delta S_p^0)/RT)$, where $K_p(T)$ is the equilibrium constant for polymerization, ΔH_p^0 and ΔS_p^0 are the enthalpy and entropy of polymerization of the monomer in the standard state, and R is the gas constant. Likewise, the quantity $K(0)$ can be identified as $K(0) = 4T_1/T$, a measure of the solvent–monomer interaction energy, related to the Flory interaction parameter,[17] χ. The variable T_1 can be considered as the mean field temperature of the upper critical solution point of the solvent–monomer solution.

The magnetic variables m and h are related[7,20] to the mole fraction of polymer, x_p, which is, in turn, related to the mole fraction of initiators, x_i. For the α-methylstyrene/sodium naphthalide system under study here, in which two initiator molecules are used to initiate each polymer molecule, $x_p = x_i/2$. From equation 3.13 of ref 7

$$h = 2x_p/m = x_i/m \tag{4}$$

From eq 5.28 of ref 20b

$$m^2 = 2x_m(x_m^* - x_m) \tag{5}$$

From eqs 6–8 of ref 20a

$$x_m(T) = x_m^* - x_p/(1 - K_p(T)\,x_m(T)) \tag{6}$$

a quadratic equation for $x_m(T)$, the mole fraction of unreacted monomer at equilibrium at T. Equation 6 is derived for a system in which one initiator molecule reacts with one monomer molecule to form the smallest propagating species. For the system we consider here of α-methylstyrene initiated by sodium naphthalide, two initiators react with two monomers to form the smallest propagating species, and the equation for x_m has a slightly different form:[13,29]

$$x_m(T) = x_m^* - x_p[2 - K_p(T)\,x_m(T)]/[1 - K_p(T)\,x_m(T)] \tag{7}$$

but is still just a quadratic equation in x_m.

Equation 3 has been used previously to interpret the neutron scattering from polymerizing sulfur solutions.[30]

In the unpolymerized region, for the limits $h \rightarrow 0$ and $m \rightarrow 0$, $K_p(T) < K_p(T_p)$. In this region, $S(q,T)^{-1}$ has an Ornstein–Zernike form (as expected from a mean field approximation):

$$S_m(q,T)^{-1} = (-4T_1/T) + [x_m^*(1 - x_m^*)]^{-1} + (4T_1a^2q^2/6T) \tag{8}$$

Likewise, in the polymerized region for $h \rightarrow 0$, $K_p(T) > K_p(T_p)$, but $m \neq 0$. When $K_p(T) \sim K_p(T_p)$, $m \rightarrow 0$ as $(K_p(T) - K_p(T_p))^{1/2} \sim (T_p - T)^{1/2}$. Then we get

$$S_p(q,T)^{-1} = (-4T_1/T)(1 - a^2q^2/6) + (1 - x_m^*)^{-1} + [a^2q^2(^1/_2 + 1/m^2J^2(0))/6x_m^*] \quad (9)$$

(a) Structure Function at $q = 0$, $S(0,T)$, in the Mean Field Approximation. In the limit $q \to 0$, we obtain from eq 3 the concentration susceptibility, $S(0,T)$,[30]

$$S(0,T)^{-1} = (-4T_1/T) + (1/x_m^*(1 - x_m^*)) - [K_p(T)(K_p(T)m + h)^3]/[(1 + {}^1/_2(K_p(T)m + h)^2)((K_p(T)m + h/2)(K_p(T)m + h)^2 + h)] \quad (10)$$

which can be shown to be exactly the eq 1 of our previous paper.[15]

We get the two limits for the case $h \to 0$:

$T > T_p$, $K_p(T) < K_p(T_p)$, $h \to 0$, $m \to 0$:

$$S_m(0,T)^{-1} = (-4T_1/T) + [1/x_m^*(1 - x_m^*)] \quad (11a)$$

$T < T_p$, $K_p(T) > K_p(T_p)$, $h \to 0$, $m \neq 0$:

$$S_p(0,T)^{-1} = (-4T_1/T) + [1/(1 - x_m^*)] \quad (11b)$$

Thus in the limit $h \to 0$, $S(0,T)$ has a discontinuity at T_p, jumping from $x_m^*(1 - x_m^*)/[1 - (4T_1/T)x_m^*(1 - x_m^*)]$ to $(1 - x_m^*)/[1 - (4T_1/T)(1 - x_m^*)]$. The effect of increasing T_1 is to increase $S_p(0,T)$, while $S_m(0,T)$ remains nearly the same. When $h \neq 0$, which corresponds to $x_i = rx_m^* \neq 0$, there is a rounding effect of $S(0,T)$ near the transition.

(b) Correlation Length from $S(q,T)$ in the Mean Field Approximation. From eq 9 for $h = 0$, we compare to the Ornstein–Zernike form $S^{-1}(q) = S^{-1}(0)[1 + q^2\xi^2]$ and define a correlation length, ξ, such that

$$\xi^2(T) = (a^2/6)[(4T_1/T) + (1/x_m^*)(^1/_2 + 1/m^2J^2(0))]/[(-4T_1/T) + (1/(1 - x_m^*))] \sim m^{-2} \quad (12)$$

when $m \to 0$. Close to the polymerization transition, we recover the classical theory result:[31]

$$\xi \sim m^{-1} \sim (T_p - T)^{-\nu} \quad \text{with } \nu = {}^1/_2 \quad (13)$$

For $h \neq 0$, for the limit $q \to 0$, we write eq 3 in the Ornstein–Zernike form and obtain

$$\xi^2(T) = S(0,T)(a^2/6)[4T_1/T + A(mJ(0))(mJ(0) + h)^2/(x_m^*((mJ(0) + h/2)(mJ(0) + h)^2 + h))] \quad (14)$$

where

$$A = 1 + [mJ(0)(1 - {}^1/_2(mJ(0) + h)^2)]/[(mJ(0) + h/2)(mJ(0) + h)^2 + h] \quad (15)$$

B. Structure Function at $q = 0$, $S(0,T)$, and the Correlation Length, $\xi(T)$, from a Non-Mean Field Approach. The theories discussed above for $S(q,T)$ for a living polymer solution assume a mean field environment and neglect fluctuations in concentration. We know that such fluctuations are important and can lead to behavior not included in mean field calculations, but we cannot do the statistical mechanics of the $n \to 0$ magnet model for the general case, including the fluctuations. Recently, however, Wheeler and Pfeuty[19] have shown that calculations of $S(0,T)$ and $\xi(T)$ can be done for the special case in which the energy of mixing between the solvent and the monomer is set at zero. That is, $T_1 = 0$ in this special case.

In the limit $h \sim x_i \to 0$, the $T_1 = 0$ limit of the dilute $n \to 0$ model predicts that $S(0,T)$ has a renormalized, weak singularity near T_p:

$$S(0,T) \sim (T_p - T)^{-\alpha/(1-\alpha)} \quad (16)$$

where α is the critical exponent for the specific heat.[31] The correlation length diverges with the renormalized critical exponent, ν:

$$\xi(T) \sim (T_p - T)^{-\nu/(1-\alpha)} \quad (17)$$

for $T < T_p$ (polymerized region). There is no singularity in $\xi(T)$ for $T > T_p$ because its amplitude is zero. The critical exponents α and ν are those of the $n \to 0$ magnet: $\alpha = 0.235 \pm 0.005$ and $\nu = 0.5885 \pm 0.0025$.[32]

Values of $S(0,T)$ and $\xi(T)$ for $h \sim x_i \neq 0$ may be calculated using eqs 5 and 12 in Wheeler and Pfeuty,[19] solving numerically for the parametric variables, from which the variables of interest may be calculated.[14] The calculation of $S(0,T)$ from eq 13 of ref 19 requires a function $F(\theta^2)$ which was not given in ref 19 but which was provided to us by the authors:

$$F(\theta^2) = [2\beta\delta(1 - \theta^2) - (1 - \alpha)(1 - 3\theta^2)]/[(1 - b^2\theta^2)(1 - 3\theta^2) + 2\beta\delta b^2\theta^2(1 - \theta^2)] \quad (18)$$

where the symbols are various critical exponents and parameters, as defined in ref 19. The calculation of $\xi(T)$ from eq 14 of ref 19 requires a function $\xi_0(\theta^2)$; following Wheeler and Pfeuty, we will take ξ_0 as a constant. For $x_i \neq 0$, there is a rounding of the divergences of $S(0,T)$ and $\xi(T)$ as compared to the case $x_i = 0$. However, if x_i is not too large, $S(0,T)$ is predicted to have a maximum in the temperature region below T_p. This maximum is not obtained in the mean field treatment of $S(0,T)$ discussed above.

C. Predictions of $S(0,T)$ and $\xi(T)$ from the Theories of Dilute and Semidilute Polymer Solutions. We have considered above the predictions of theories of living polymer solutions which are based on models of equilibrium polymerization as a phase transition. Living polymer solutions may also be considered in the context of the models of polymer solutions in general. Just below the polymerization temperature, a living polymer solution can be viewed as a dilute solution of noninteracting, polydisperse polymer molecules. As the temperature decreases further, the living polymer molecules grow larger, and eventually the largest polymer molecules will begin to interpenetrate. Then the living polymer solution can be viewed as a semidilute solution of polydisperse, linear polymer molecules. Other complications can arise because the living polymer molecules are carbanions, having negative electrical charges at the active ends and associated with counterions in the polar organic solvent.[1,3] We note also that neither the temperature nor the volume fraction of living polymers in the solution is held constant in our experiments.

At equilibrium, the living polymer molecules are expected to have a broad molecular weight distribution.[33] We are aware of no published experimental study of the equilibrium molecular weight distribution of this living polymer solution. We have made preliminary measurements[13] of the time development of the molecular weight distribution at a given temperature for the same α-methylstyrene system we study here, and we have more extensive experiments underway.[34]

The models of terminated ("dead") polymer molecules in solution fall into the same two categories discussed above for living polymer solutions: mean field models and non-mean field ("scaling") models. These models provide equations for the power law behaviors of various thermodynamic properties of interest. These models are expected to be perfectly consistent with the models in parts A and B above, mean field with mean field and non-mean field with non-mean field.

For a *dilute* solution of "dead" polymers, the correlation length, ξ, as obtained from the scattering of radiation in the regime $q\xi \ll 1$, is a measure of the radius of gyration,[35] R_G. From the scaling approach to polymer solutions,[36] the expected behavior in a dilute solution of monodisperse polymer molecules is

$$\xi \sim R_G \sim M^{\nu} = \mathrm{DP}^{\nu} \quad \text{(dilute; good solvent)} \quad (19)$$

where M is the number-average molecular weight, DP is the number-average degree of polymerization (the number of monomers in a polymer), and ν is the same critical exponent given above. For such a dilute solution, ξ does not depend on the concentration of the polymer molecules, since they are not interacting. However, eq 19 holds only for large, flexible polymer molecules (DP > 300).[37] The exponent describing the dependence of R_G on DP is expected to be larger (as large as 1) for stiffer or shorter chains.[38] In the case of a living polymer solution in the dilute regime, ξ should *increase* as the temperature falls below T_p and the average molecular weight of the polymers increases. However, as we shall see below, DP in our experiments reaches only about 100 before the transition to a semidilute regime. Thus, we do not expect eq 19 to hold because of the small DP of the living polymers in the dilute regime of our experiment. Moreover, a proper calculation of R_G from scattering data requires an extrapolation to zero concentration at fixed M, which is not possible for our experiments, in which M depends on T and on the volume fraction of polymer. Finally, solutions of living polymers are not monodisperse, as discussed above. Thus we will not attempt to apply eq 19 to our measurements. Likewise, $S(0)$, the measured structure function at $q = 0$, for a "dead" polymer in the dilute region is a measure of the dependence of the osmotic pressure on concentration and of the average molecular weight;[39] we will not analyze our data in these terms, for the same reasons listed for ξ.

As either the concentration of polymer molecules or the average molecular weight of the polymer molecules in a solution of "dead" polymers is increased, the molecules will eventually overlap, at which point the polymer solution enters the *semidilute* regime. For this regime, there is a macroscopically uniform distribution of chains in the solvent and the system can be viewed as a mesh of polymer chains.[36] The correlation length, ξ, as obtained from the scattering of radiation such that $q\xi \approx 1$, will be the size of the mesh.[39] Experiments on "dead", monodisperse polymer chains in solution confirm the theoretical prediction that the correlation length depends on the volume fraction, ϕ_v, of polymer as[21,22,36,39]

$$\xi \sim \phi_v^{-\nu/(3\nu-1)} \sim \phi_v^{-0.77} \quad \text{(semidilute; good solvent)} \quad (20)$$

Earlier mean field calculations predicted $\xi \sim \phi_v^{-0.5}$ for a semidilute polymer solution in a good solvent.[25] For a solution of "dead", monodisperse polymer chains in the semidilute region, $S(0)$, the structure function at $q = 0$, is expected[39] from scaling arguments to vary as $\phi_v^{-0.25}$ and to be independent of molecular weight. Mean field arguments predict[39] $S(0)$ to be independent of both concentration and molecular weight.

For the living polymer solutions we study here, we expect $\xi(T)$ to begin to *increase* as the temperature is lowered through the polymerization temperature and polymers start to grow. When the largest polymers begin to overlap, $\xi(T)$ will begin to *decrease* as the mesh is formed and becomes "finer". Thus the maximum in $\xi(T)$ for a living polymer solution will indicate the point of overlap and the onset of the semidilute regime; we will indicate the degree of polymerization at overlap as DP* and the volume fraction of polymer at overlap as ϕ_v*. We see that the situation will be complicated by the polydispersity: the first chains to interpenetrate will be the largest ones.

Table 1. Samples of Living Poly(α-methylstyrene) in Tetradeuteriofuran, Initiated by Sodium Naphthalide[a]

sample	x_m*	c_m* (g/cm³)	$r \times 10^3$	T_p (K)	$p_{max} \times 10^{-3}$
91-1	0.12 ± 0.01	0.16	3.9 ± 0.5	282 ● 2	0.51
91-3	0.049 ± 0.004	0.072	10 ± 1	266 ± 2	2.0
92-1	0.0526 ± 0.0003	0.076	9.3 ± 0.3	266 ± 2	2.2

[a] The mole fraction of initial monomer is x_m*, the total number of grams of monomer per cm³ of solution is c_m*, the ratio of moles of initiator to moles of initial monomer is r, and the experimental polymerization temperature is T_p (taken as the temperature at which scattering begins). The maximum possible degree of polymerization is p_{max}: the number of monomers per polymer if all the monomer were fully encorporated into polymer; $p_{max} = 2r^{-1}$. Uncertainties are given at the 99% confidence interval.

III. Experimental Methods

A. Sample Preparation. The starting materials were 99.5% deuterated tetrahydrofuran (TDF) from Sigma Chemical Co., 99.9% pure hydrogenated tetrahydrofuran (THF) from Aldrich Chemical Co., 99% pure α-methylstyrene from Aldrich Chemical Co., 99% pure naphthalene from Baker Chemical Co., and 99.95% pure sodium from Aldrich Chemical Co.

All materials were rigorously degassed and dried to prevent water and oxygen from terminating the polymer molecules. Our purification and handling techniques are described in detail in refs 8–14. In these techniques, all manipulations are carried out on a vacuum line or in an argon drybox (at <5 ppm oxygen or water). In the present work, the TDF and THF were first dried with P_2O_5. The subsequent drying and distillation procedures for TDF and THF were the same as those reported previously for THF. The sodium naphthalide initiator was prepared by placing massed quantities of sodium and naphthalene (with a slight excess of sodium) in a flask in the drybox, adding clean THF to the flask, and swirling the flask every 15 min for 2 h. This THF solution was diluted with TDF before use, and then only a small amount was used in the sample, so the amount of THF in the final sample was insignificant.

The quartz neutron scattering cells (made by Hellma Co.) were quartz disks with a sample thickness (neutron path) of 2.5 mm, a wall thickness of 0.5 mm, and a diameter of 21.5 mm.

The three samples are described in Table 1. Samples 91-1 and 91-3 were prepared in 1991 by one of us.[13] Sample 92-1 was prepared a year later by another of us.[14] Samples 91-3 and 92-1 are very similar in x_m* and in r. Sample 91-3 was made by putting the required volume of clean THF into a reaction vessel attached to the neutron scattering cell,[12] adding the required volume of clean α-methylstyrene, and then adding the required volume of initiator solution. This solution was *not* degassed by freezing, pumping, and thawing[13] because we now believe that it is important that the samples never be cooled below the polymerization temperature before we begin studying them, so that no metastable or dead polymers can possibly be present on the first experimental cooling run (see below). The solution was then poured from the reaction vessel into the cell, and the cell was permanently sealed. Sample 91-1 was made from residual mixture

from sample 91-3: a quantity of sample 91-3 was transferred to a new and clean reaction vessel (attached to a neutron scattering cell), and an appropriate quantity of clean α-methylstyrene was added to it. Sample 92-1 was prepared in essentially the same way, except that the procedure was simplified: no reaction vessel was attached to the cell, but instead the cell was sealed with a septum, through which the materials were injected.

Sealing the neutron cells was a delicate task: the sealing had to be done at a Pyrex section of the cell neck—not on the quartz part because quartz requires very high temperatures to melt and seal; the cell (still attached to the reaction vessel) was evacuated very slightly to make sealing easier; the cell and the reaction flask were held in cold water just above the polymerization temperature to prevent sample loss during sealing.

B. SANS Apparatus and Temperature Control. The SANS experiments were performed on the spectrometer PACE in the reactor Orphée at the Laboratoire Léon Brillouin (CEA–CNRS), Saclay, France. The incident wavelength, λ, obtained by a mechanical selector, was 6.5 Å ± 10% for samples 91-1 and 91-3, and 6.0 Å ± 10% for sample 92-1. The q range of the collimated beam was 9.6×10^{-3} to 0.10 Å^{-1}. The standard deviation of the measured intensity was about 0.025 cm^{-1}.

The cells were held in the neutron beam in an aluminum block, the temperature of which was controlled to ±0.1 K by circulating an ethylene glycol–water mixture. The temperature was measured by means of a platinum resistance thermometer, placed in the aluminum block.

C. Procedures. As noted above, the samples were never allowed to cool below the polymerization temperature, T_p, before being placed in the spectrometer and deliberately cooled, in temperature steps of 0.1–1 K. For samples 91-1 and 91-3, at each temperature on the initial cooling runs, three spectra were taken, each with a collection time of 10 min. Since the temperature was not yet stable for the first spectrum, only the latter two spectra at each temperature of the cooling run were summed and analyzed. Those two spectra agreed with one another, indicating that, for the initial cooling run, equilibrium was attained in the polymer solution within the collection time of the first spectrum.

For sample 91-1, the first heating run did not reproduce the initial cooling run. For the heating run, the intensity at any particular temperature was always higher than had been recorded for the same temperature during the initial cooling run, and the intensity continued to decrease with time, even after periods as long as 2 h, never reaching the value recorded on the initial cooling run.[13] Then the sample was inadvertently heated to 313 K. This "annealing" had a very interesting effect: the scattering intensities measured on the initial cooling run were then reproduced on the second cooling run! The data from the first (initial) and second cooling runs of sample 91-1 are included in our analysis.

For sample 91-3, the cooling run was likewise followed by a heating run, during which data were taken at the same time and temperature intervals as for the cooling run. As for sample 91-1, the data taken on heating had higher scattering intensities than the data taken on the initial cooling.[13] We conclude that data taken after the first cooling for sample 91-3 do not represent equilibrium data, and we do not analyze those data here.

For sample 92-1, spectra were taken at 5-min intervals and for time periods up to 11 h, in an effort to understand better the equilibration times required.[14] The sample was first cooled slowly from 292 to 268 K, at which point the scattering intensity began to increase and we began collecting spectra. In contrast to the procedures for samples 91-1 and 91-3, for which the temperature was steadily decreased in steps for the initial cooling run, for sample 92-1, the temperature was alternately decreased and increased in small steps (0.2–0.7 K). Thus the sample was alternately heated and cooled on the initial "cooling" run. Our intention was to collect spectra for both heating and cooling steps on the initial "cooling" run, in order to observe any differences in the equilibration kinetics between heating and cooling. After the initial cooling to 250.9 K, the sample was then warmed to room temperature over 5.5 h; data were not collected during the warming. As shown in Figure 1, the spectrum taken at 291.2, taken 4.4 h after the spectrum at 250.9 K, is virtually identical to the spectrum taken at the start of the run at 282.9 K (over 3 days earlier), indicating complete reversibility of the polymerization. All the data from this initial run are analyzed here.

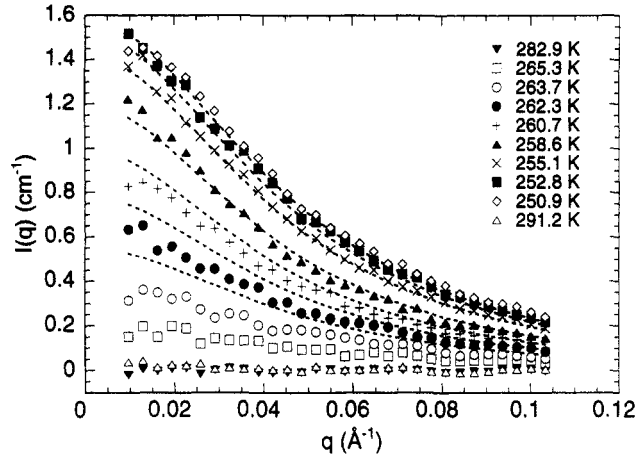

Figure 1. Representative coherent neutron scattering intensity $I(q,T)$ spectra for sample 92-1 of living poly(α-methylstyrene) in TDF as a function of wavenumber, q, and temperature, T. The polymerization temperature, T_p, is 266 ± 2 K. Note the absence of scattering above T_p and the increased scattering as the temperature decreases below T_p and the living polymers grow. The dashed lines represent the predictions of the mean field theory, using eq 3 and the parameters described in the text.

Spectra were collected at 66 temperatures for the initial cooling of sample 91-1, at 41 temperatures for the second (annealed) cooling of sample 91-1, at 93 temperatures for the initial cooling of sample 91-3, and at 100 temperatures for sample 92-1.

D. Data Reduction. Two or more scattering spectra at each temperature were combined[14] to obtain the "raw intensity", $I_r(q,T)$. $I_r(q,T)$, was corrected in a standard way[12-14] for the scattering from the empty cell walls and scaled by the scattering cross-section of 1 mm of water (taken[40] to be 0.87 cm^{-1} at 6.5 Å for samples 91-1 and 91-3 and taken to be 0.85 cm^{-1} at 6.0 Å for sample 92-1) to obtain $I'(q,T)$. This corrected and scaled $I'(q,T)$ still contains incoherent background scattering. We correct for this background by subtracting from $I'(q,T)$ the value of the background scattered intensity, $I_b(q,T_b)$. For samples 91-1 and 91-3, $I_b(q,T_b)$ was taken as the scattering spectrum for a "blank" solution—a solution containing monomeric α-methylstyrene in TDF, but with no initiator present—at 269 K. For sample 92-1, $I_b(q,T_b)$ was taken as the scattering spectrum for the sample itself at 284.3 K, before it had ever been cooled below T_p. Thus we obtain

$$I(q,T) = I'(q,T) - I_b(q,T_b) \tag{21}$$

where we note that the background spectrum was recorded at only one temperature but was applied at all temperatures.

Rather than covert the data from the corrected intensity spectra into spectra of the concentration structure function, $S(q,T)$, we convert the theoretical calculation of $S(q,T)$ into $I(q,T)$ using the constrast,[41] κ:

$$I(q,T) = \kappa(S(q,T) - S_b(q,T_b)) \tag{22}$$

where $S_b(q,T_b) = S_m(q,T_b)$, as given in eq 8, and where

$$\kappa = (1/V)[b_2(V_1/V) - b_1(V_2/V)]^2 \tag{23}$$

in which V_1 (=2.18 × 10^{-22} cm^3/molecule) and V_2 (=1.33 × 10^{-22} cm^3/molecule) are the respective molecular volumes for the α-methylstyrene and the TDF, V is the mean molecular volume ($V = x_m^* V_1 + (1 - x_m^*)V_2$), and b_1 (=2.245 × 10^{-12} cm) and b_2 (=8.580 × 10^{-12} cm) are the respective coherent molecular neutron scattering collision lengths. We obtain κ = 0.83 cm^{-1}.

IV. Results and Discussion

A. $I(q,T)$. Figure 1 shows typical neutron scattering spectra $I(q,T)$ for a sample of living poly(α-methylstyrene) in TDF, as recorded at several temperatures on the initial cooling run of sample 92-1. Note the lack of scattering at

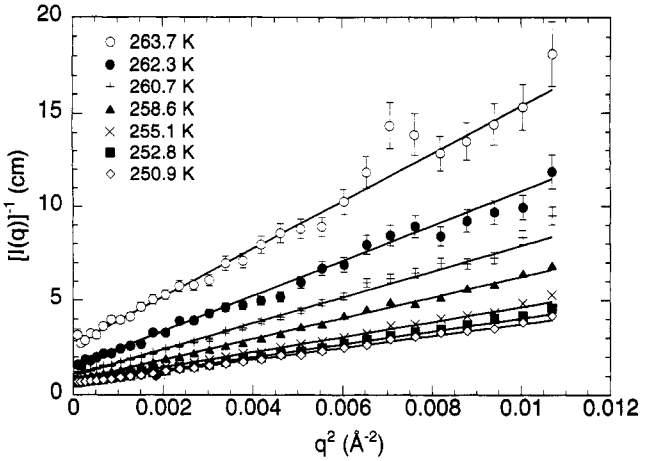

Figure 2. Inverse of $I(q,T)$ plotted versus q^2 for representative spectra for sample 92-1 of living poly(α-methylstyrene) in TDF. The solid lines are functions fitted to the Ornstein–Zernike function (eq 24).

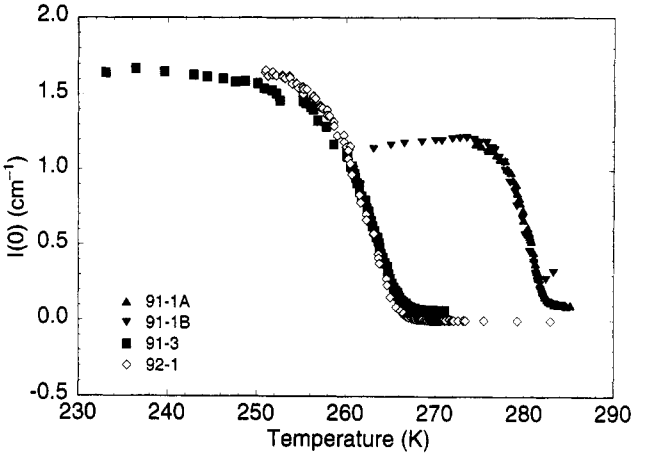

Figure 3. Intensity at $q = 0$, $I(0,T)$, for samples of living poly(α-methylstyrene) in TDF. The symbols are the experimental values of $I(0,T)$ as obtained by fits to eq 24. The legend identifies the samples; A and B refer to the initial and second cooling runs.

temperatures above the polymerization temperature of 266 ± 2 K. The scattering intensity then increased dramatically as the temperature was decreased, reflecting the growth of the living polymers.

We have fitted eq 3 for $S(q,T)$ in the mean field approximation to some representative $I(q,T)$ spectra. These fitted functions are also shown in Figure 1. The values of the parameters used are $\Delta S_p = -105$ J/(mol K), $\Delta H_p = -34.6$ kJ/mol, $T_1 = 37$ K, and $r = 0.010$; these values were determined, as discussed below, from the best fits to the mean field expressions for $S(0,T)$. The only free parameter in the $S(q,T)$ calculation was the monomer size, "a", which was adjusted to 10.19 Å for the best fit. The comparison in Figure 1 of the mean field theory for $S(q,T)$ with our experimental spectra shows relatively good agreement.

B. $I(0,T)$. Figure 2 shows $1/I(q,T)$ plotted versus q^2 for some representative spectra for sample 92-1. The linearity of these plots justifies fitting the data to an Ornstein–Zernike type expression:

$$I(q,T) = I(0,T)/(1 - q^2\xi^2(T)) \qquad (24)$$

We also tested the addition[13] of a term $\epsilon(T)$ to eq 24 to account for such contributions as multiple scattering, the thermal expansion of the solvent, etc.: i.e., to adjust for the fact that we cannot completely determine the background correction, $I_b(q,T)$. We allowed $\epsilon(T)$ to be a free parameter; the resulting values of $\epsilon(T)$ were typically only about 5% of the intensity. The fitted values for $I(0,T)$ and for $\xi(T)$ were not changed significantly when $\epsilon(T)$ was set at zero, so we present our analysis without the term $\epsilon(T)$.

We have fitted eq 24 to all the spectra $I(q,T)$ for all the samples, allowing $I(0,T)$ and $\xi(T)$ to be free parameters at each temperature and using a weighted least squares fitting routine which takes into account the correlations among free parameters.[14] We report the errors at the 99% confidence interval. These fitted parameters are listed in ref 14 for all three samples.

The solid lines in Figure 2 are represented of the functions fitted to eq 24 and confirm the validity of our use of eq 24. We note that eq 24 is derived from mean field models.[39,42] Thus our use of eq 24 to obtain the physically interesting quantities $I(0,T)$ and $\xi(T)$ could bias these quantities toward mean field behavior, when we wish to compare these quantities to both a mean field theory and a non-mean field theory. We know, however, that deviations from eq 24 are very small even at critical points in fluids of small molecules,[43] which are much more strongly non-mean field than are polymer solutions.[44] We therefore assume that the use of eq 24 will not significantly bias the values of $I(0,T)$ and $\xi(T)$, and our discovery of behavior for $I(0,T)$ which is clearly non-mean field (see below) supports this assumption.

$I(0,T)$ as determined from these fits is plotted as a function of temperature for all the samples in Figures 3 and 4. Recall that sample 92-1 was meant to duplicate 91-3 and was made and studied a year later by a different person. We note the good agreement between samples 91-3 and 92-1: T_p is the same for both samples, and the transition is somewhat "sharper" for 92-1, due to the slightly smaller value of r (see Table 1). We note also the dramatic rise of $I(0,T)$ when the temperature falls below the polymerization temperature. For samples 91-3 and 92-1, $I(0,T)$ then levels off at lower temperatures. However, for sample 91-1, $I(0,T)$ shows a maximum as the temperature decreases below T_p; this is a significant feature which we shall discuss below.

We compare the experimental $I(0,T)$ data to the predictions of mean field theory (eq 10 above) in Figure 4. The free parameters of the theoretical functions were obtained using the computer program MATLAB,[45] which provides a Nelder–Meade (modified) simplex minimization of the residuals between the data and a function of several variables.[46] We first set x_m^* and r at their experimental values (Table 1) and allowed $\Delta H_p°$, $\Delta S_p°$, and T_1 to vary within the uncertainties of the literature values[8,47] (see Table 2) to obtain the best values of $\Delta H_p°$, $\Delta S_p°$, and T_1 which simultaneously described all three samples. We note that in the mean field calculation, T_p is determined by $\Delta H_p°$, $\Delta S_p°$, and x_m^* and is not an independent parameter. Those best fit values are given in Table 2. The uncertainties given in Table 2 for the fitted parameters were determined by testing for the effect on the parameters of allowing the reduced χ^2 to increase by an amount corresponding to a 99% confidence interval.[48] The value of T_1, the mean field upper critical solution temperature for the solution of monomer in solvent, seems reasonable, TDF being a good solvent for α-methylstyrene. Then these three parameters were fixed at their best values, x_m^* was set at the experimental value for each sample, and r for each sample was allowed to vary to optimize the fit of the theory to the data. The final values of r are also given in Table 2. The fitted values of r are in reasonable agreement with the experimentally determined values; we note that

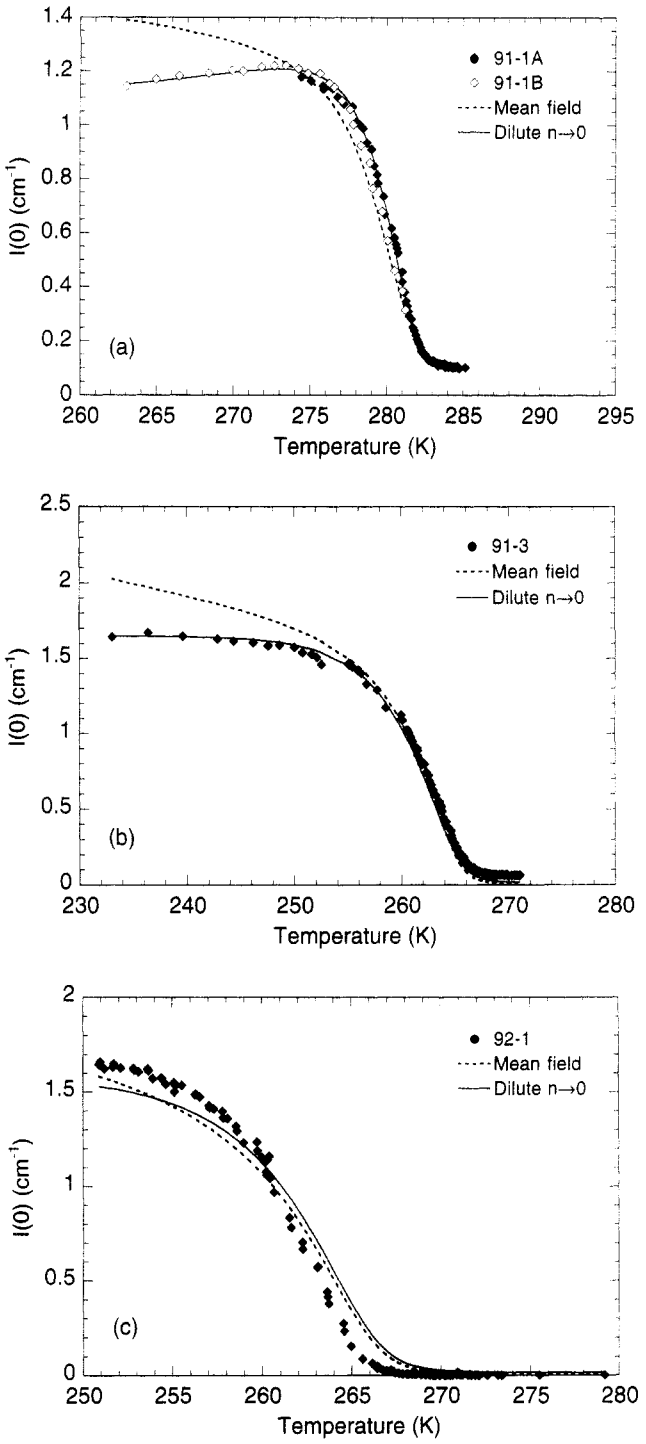

Figure 4. Intensity at $q = 0$, $I(0,T)$, for samples of living poly(α-methylstyrene) in TDF. The symbols are the experimental values of $I(0,T)$ as obtained by fits to eq 24. For sample 91-1, A and B refer to the initial and second cooling runs. The theoretical predictions for the mean field theory (eq 10) using the parameters discussed in the text are shown as dashed lines. The theoretical predictions for the non-mean field, dilute $n \rightarrow 0$ magnet theory[19] using the parameters discussed in the text are shown as solid lines.

some of the initiator molecules could have been deactivated during the sample preparation, so that the experimental values of r must be upper limits to the fitted values of r.

We also tested the sensitivity of the mean field theory to changes in the fitted parameters.[14] The predictions are not very sensitive to changes in T_1 or r. However, the fits are quite sensitive to changes in $\Delta H_p°$ (a 1% change in $\Delta H_p°$ changes $I(0,T)$ by a factor of 2–3) and quite sensitive to changes in $\Delta S_p°$ (a 1% change in $\Delta S_p°$ changes $I(0,T)$ by a factor of about 2).

The resulting predictions of the mean field theory for $I(0,T)$ using the best fit values of the four fitted parameters are compared to the experimental data in Figure 4. Keep in mind in studying Figure 4 that sample 92-1 is essentially the same as sample 91-3, except that the data were taken over a smaller temperature range. Thus the apparently better agreement between the mean field theory and sample 92-1 is due to the fact that the temperature range is smaller. The mean field theory clearly predicts the correct qualitative behavior for $I(0,T)$, but it also clearly is not quantitatively accurate. In particular, it fails to predict the maximum in $I(0,T)$ below T_p, at sufficiently low r, as is seen for sample 91-1.

We next compare $I(0,T)$ to the predictions of the dilute $n \rightarrow 0$ magnet model.[19] For these equations, the MATLAB Nelder–Mead simplex minimization routine failed to converge, so we were forced to vary the parameters stepwise to find the best fits. For the dilute $n \rightarrow 0$ magnet theory, the free parameters are r, $\Delta H_p°$, and $T_p°$, the polymerization temperature of pure α-methylstyrene. Again, best values of $\Delta H_p°$ and $T_p°$ were found in common for all three samples, after which r was varied independently for each sample. Uncertainties were determined in the same way as for the mean field theory. The fits for the dilute $n \rightarrow 0$ magnet theory are not very sensitive to $\Delta H_p°$ or r but are sensitive to $T_p°$: a 1% change in $T_p°$ shifts $I(0,T)$ by 10%.

The best fit values are given in Table 2, and the functions are plotted in Figure 4. The dilute $n \rightarrow 0$ magnet model clearly gives better agreement with the data for $I(0,T)$ than does the mean field theory. In particular, the dilute $n \rightarrow 0$ magnet model correctly predicts[19] the maximum in $I(0,T)$ below T_p for sample 91-1 (the sample with the lowest r), a feature not predicted by the mean field theory.

C. Characteristic Length, $\xi(T)$. Our fits of the $I(q,T)$ spectra to eq 24 also result in values of the characteristic length, or correlation length, $\xi(T)$. Figure 5 shows $\xi(T)$ for all samples. We see for all the samples the expected increase in ξ as the temperature passes through T_p and the polymer molecules begin to grow, a maximum at ξ^*, and an ensuing decrease in $\xi(T)$. The value of ξ^* is about the same for samples 91-1 and 91-3 but higher for 92-1. The higher, sharper maximum for sample 92-1 is, in part, due to the fact that r is smaller for sample 92-1 (see Table 1); there could also be some effect due to the different thermal history of sample 92-1, which was heated and cooled alternately. The maximum in $\xi(T)$ is related to the interpenetration of polymer chains in the system, as we discuss below.

We first compare $\xi(T)$ to the predictions of the mean field RPA theory, using eqs 14 and 15. The parameters for the mean field theory (see Table 2) for $I(0,T)$ were used for the calculation of $\xi(T)$. The additional parameter "a" was allowed to vary for each sample to obtain the best fits; the value of "a" obtained should be the same for all the samples and is the same, within the large uncertainties: 8 ± 3 Å for sample 91-1, 8 ± 2 Å for sample 91-3, and 11 ± 1 Å for sample 92-1. If we calculate the predicted functions for the highest and lowest values of "a" allowed by the error bars, then we shift the predicted curves up and down vertically on Figure 6. The mean size of the monomer, as calculated from the density of unpolymerized α-methylstyrene, is a = 6 Å, which is close to the fitted values for samples 91-1 and 91-3. The value of "a" for sample 92-1 is larger than those for 91-1 and 91-3 but is still within the combined uncertainties. This large value

Table 2. Values of Thermodynamic Parameters for the Living Polymerization of α-Methylstyrene in Tetradeuteriofuran As Obtained from the Literature and from the Best Fits to Our Data Using the Mean Field Theory (Eq 10 and the Dilute $n \to 0$ Magnet Theory[19])[a]

	ΔH_p^0 (kJ/mol)	ΔS_p^0 (kJ/(mol K))	T_1 (K)	T_p^0 (K)	$r \times 10^3$ 91-1	91-3	92-1
literature	−35 ± 1[b]	−110 ± 1[c]	34.9–37[d]	321 ± 10[c]	3.9 ± 0.5[e]	10 ± 1[e]	9.3 ± 0.3[e]
mean field	−34.6 ± 0.5	−105 ± 1	37 ± 5	NA	4 ± 2	7 ± 2	10 ± 2
dilute $n \to 0$	−35 ± 1	NA	0	329 ± 6	4.4 ± 0.7	8.3 ± 0.5	9.4 ± 0.8

[a] Uncertainties are given at the 99% confidence interval. Here ΔH_p^0 is the enthalpy of propagation of α-methylstyrene in the standard state of pure monomer, ΔS_p^0 is the entropy of propagation of α-methylstyrene in the standard state of pure monomer, T_1 is the mean field upper critical solution temperature for monomeric α-methylstyrene in TDF, T_p^0 is the polymerization temperature for pure α-methylstyrene, and r is the ratio of initial moles of monomeric α-methylstyrene to moles of initiator. Samples are indicated as 91-1, 91-3, and 92-1 (see Table I). "NA" means not applicable. [b] Reference 47. [c] Reference 8. [d] References 13 and 15. [e] Experimental value from Table 1.

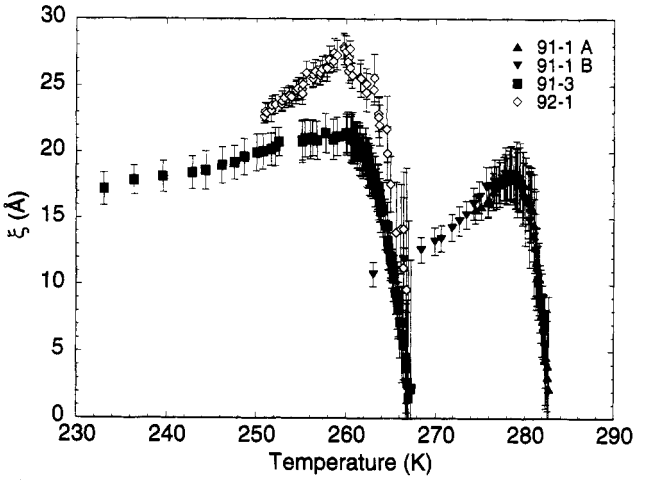

Figure 5. Characteristic length, $\xi(T)$, for samples of living poly(α-methylstyrene) in TDF. The symbols are the experimental values of $\xi(T)$ as obtained by fits to eq 24. The legend identifies the samples. For sample 91-1, A and B refer to the initial and second cooling runs.

could also be related to the different thermal history of sample 92-1, in that this sample was subjected to heating steps while it was cooled and could have contained metastably large polymers. We see from Figure 6 that the predictions of the mean field theory for $\xi(T)$ are in qualitative, but not quantitative, agreement with the experimental values of $\xi(T)$.

We next compare $\xi(T)$ to the predictions of the non-mean field, dilute $n \to 0$ magnet model, using the equations in ref 19, as discussed above. The parameters for the dilute $n \to 0$ magnet theory (see Table 2) for $I(0,T)$ were used to calculate $\xi(T)$. The additional parameter ξ_0 was allowed to vary for each sample. The parameter ξ_0, which is difficult to relate directly to the dimension of the monomer, should, in principle, have the same value for all the samples and was found to be essentially the same within the uncertainties: 1.8 ± 0.6 Å for sample 91-1, 2.1 ± 0.5 Å for sample 91-3, and 2.7 ± 0.2 Å for sample 92-1. The comments about sample 92-1 in the previous paragraph apply here as well. Figure 6 shows the comparison of the predictions of the non-mean field dilute $n \to 0$ magnet theory to the experimental values of $\xi(T)$. As for the mean field RPA theory, the agreement with the measurements is qualitative but not quantitative. The prediction of the dilute $n \to 0$ magnet theory could perhaps be improved if the assumption[19] of a constant ξ_0 in place of a function $\xi_0(\theta^2)$ were not made.

We include also in Figure 6 the conversion of the temperature axes to the fraction of initial monomer converted to polymer at each temperature, $\phi(T)$, and to the number-average degree of polymerization at each temperature, DP(T), where ϕ and DP have been calculated from the mean field theory, with the mean field values of the parameters as given in Table 2. We know from a study we have in progress in which we are measuring DP(T) for this system that the mean field theory is accurate to at least 10% at the lowest temperatures at which we took data; we believe it to be less reliable near T_p. We note that $\phi(T)$ and DP(T) are not linear in T and are related to one another as DP = $2\phi/r$. The maximum ξ^* in $\xi(T)$ occurs at $\phi^* \approx 0.2$ and DP* ≈ 100 for sample 91-1, at $\phi^* \approx 0.4$ and DP* ≈ 90 for samples 91-3, and at $\phi^* \approx 0.4$ and DP* ≈ 80 for sample 92-1. The maximum ξ^* is about 20 Å for both samples 91-1 and 91-3 and is larger (about 27 Å) for sample 92-1. We interpret the maxima as occurring at the onset of overlap, at the transition from the dilute regime to the semidilute regime. Sample 91-1 has over twice as much initial monomer and has less than half as much initiator relative to initial monomer as do samples 91-3 and 92-1. Thus all three samples have about the same mole fraction of polymers ($x_p = x_i/2 = rx_m^*/2 \sim 2.4 \times 10^{-4}$). However, sample 91-1 will have larger polymers (because r is smaller), and thus a smaller ϕ^*, which is the case (i.e., $\phi^* \approx 0.2$ for 91-1 versus 0.3 for 91-3 and 92-1). The overlap concentration $c^* = \phi^* c_m^*$ (see Table 1) is about the same for all three samples (~0.03 g/cm³), and the value of DP* is about the same for all three samples (~80–100).

An equivalent solution of monodisperse "dead" polymers with a degree of polymerization of 80 should have a much larger overlap concentration, c^*, and a much smaller correlation length at overlap, ξ^*. For example, for polystyrene in benzene[49] with DP = 80, we expect c^* = 0.23 g/cm³ and ξ^* = 5.5 Å. To get values close to those measured in our polydisperse solution of living polymers, DP for a monodisperse solution of "dead" polymers would have to be much larger: for DP = 1200, we get ξ^* = 27 Å and c^* = 0.029 g/cm³ for polystyrene in benzene. In a very polydisperse system like our living polymer system, the overlap is determined by the longest polymers, so that c^* and ξ^* cannot be obtained from the theory of monodisperse semidilute solutions with the same number-average degree of polymerization. A different averaged degree of polymerization must be considered, where the longest polymers are more heavily weighted.

In Figure 7, we plot log(ξ) versus log(ϕ) for all the samples, where again ϕ is calculated from the mean field theory. Since ϕ is proportional to DP and DP is proportional to the number-average molecular weight, M, a power law behavior $\xi = M^z \sim \mathrm{DP}^z \sim \phi^a$ would result (see eq 19) in a straight line on this log–log plot. Clearly, the behavior can be said to follow a simple law only in limited regions, at very low ϕ or at high ϕ. The broad transition region (from dilute to semidilute behavior) does not show simple power law behavior at all. The large error bars at low ϕ preclude the determination of a slope. At the highest ϕ, the slope is smaller than the −0.77 expected.

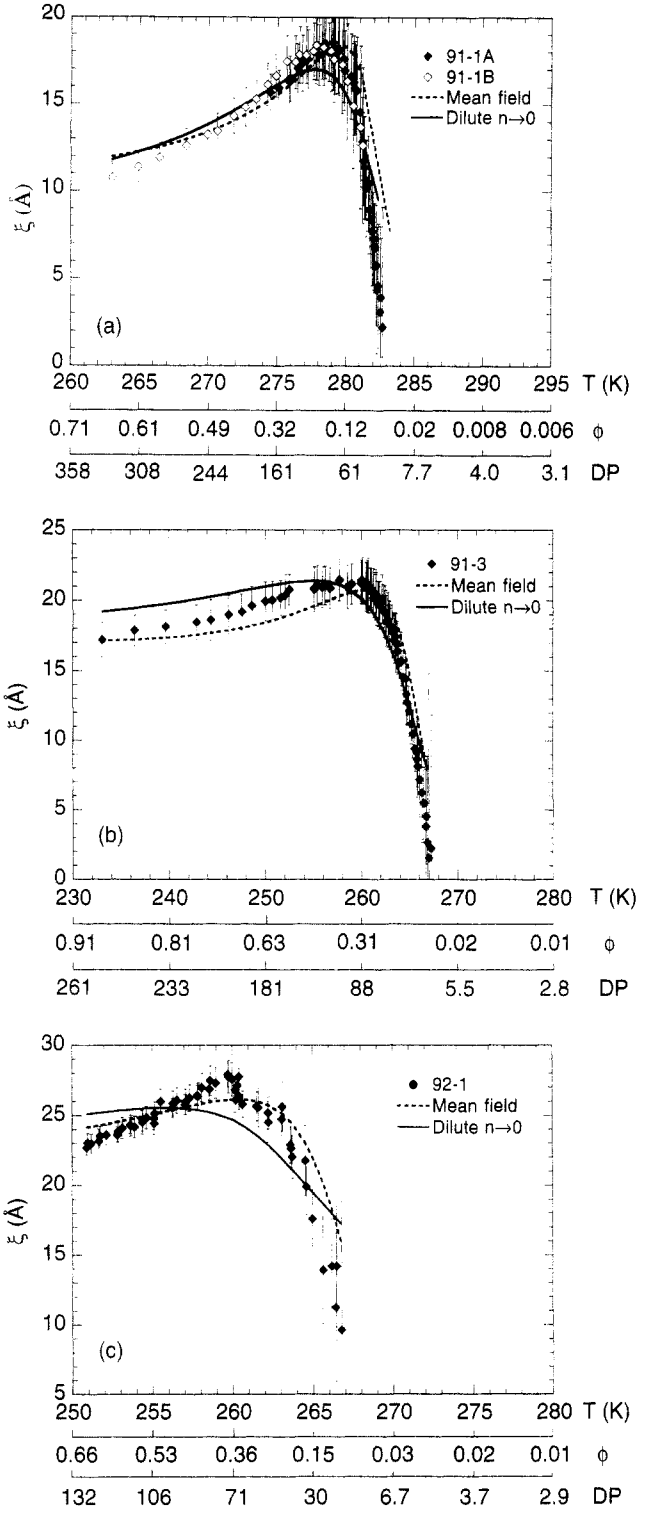

Figure 6. Characteristic length, $\xi(T)$, for samples of living poly(α-methylstyrene) in TDF. The symbols are the experimental values of $\xi(T)$ as obtained to fits by eq 24. The legend identifies the samples; for sample 91-1, A and B refer to the initial and second cooling runs. The theoretical predictions for the mean field theory (eq 14) using the parameters discussed in the text are shown as dashed lines. The theoretical predictions for the non-mean field, dilute $n \rightarrow 0$ magnet theory[19] using the parameters discussed in the text are shown as solid lines. The axes also indicate the fraction of monomer converted to polymer, ϕ, and the number-average degree of polymerization, DP, as calculated from the mean field theory.

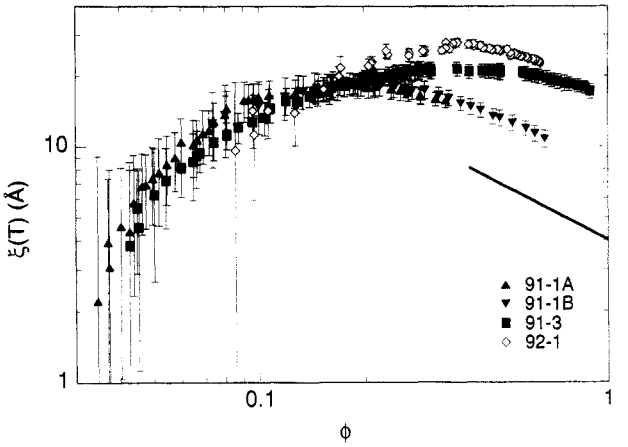

Figure 7. Logarithm to the base 10 of the characteristic length, $\xi(T)$, for samples of living poly(α-methylstyrene) in TDF plotted as a function of the logarithm to the base 10 of the fraction of initial monomer converted to polymer, ϕ, as calculated from the mean field theory. The symbols are the experimental values of $\xi(T)$ as obtained by fits to eq 24. The legend identifies the samples; for sample 91-1, A and B refer to the initial and second cooling runs. The quantity ϕ is directly proportional to the number-average molecular weight of the living polymer. The solid line at the right of the figure indicates a slope of −0.77 (see discussion in text).

IV. Conclusions

We report here the first extensive study by SANS of an organic living polymer system, evolving as a function of temperature and presenting a polymerization transition. As difficult as it is to make stable samples of these systems, we have been able to make consistent SANS measurements, using samples made by two different persons a year apart. The measurements of the structure function, $S(q,T)$, of $S(0,T)$ (its limit for $q = 0$) and of the characteristic length, $\xi(T)$, are all in remarkably good qualitative agreement with two theories which model the onset of equilibrium polymerization as a phase transition. The first theory, an RPA mean field theory, is developed in this paper. The second theory, which was stimulated by the present experiments, is a non-mean field approach, based on the renormalization group study of the $n \rightarrow 0$ magnet model. For $S(0,T)$, the non-mean field theory shows the maximum below T_p which we observe experimentally and which is not predicted by the mean field theory. For $\xi(T)$, both theories predict a peak in $\xi(T)$ below T_p, which we clearly observe experimentally. There is still a lack of a quantitative theory to describe the experimental results. However, even the qualitative success of these theoretical models is gratifying, given that the theories were developed for phase transitions in magnets and are applied here to equilibrium polymerization and given the small number of free parameters in the models.

These solutions of living poly(α-methylstyrene) seem to reach the point of overlap at smaller concentrations than do solutions of more nearly monodisperse, terminated polymers with the same number-average degree of polymerization. However, as discussed in section IIc, living polymer systems at equilibrium have a broad distribution of molecular weights.[33] The presence of some very large polymers must affect strongly the concentration at overlap, pushing the overlap concentration to lower values. The polydispersity could also have a rounding effect on the dependence of ξ on the concentration, so that the predicted power law behavior of −0.77 is difficult to see unless the concentration of initiators is smaller, so that the polymers are longer at overlap. Stable solutions with such small initiator concentrations are difficult to prepare. In addition, the exponent −0.77 is applicable at concentrations somewhat larger than those studied here.[50]

It is also probable that the low values of the overlap concentrations for these living polymer solutions are

related to the ionic nature of the living polymer molecules. It is known that polyelectrolytes show low overlap concentrations, because the Coulombic repulsion causes stretching of the polymer molecules.[51]

The observation that the samples did not reach equilibrium on heating within the same periods of time required for equilibration on cooling is consistent with our earlier observations that the "best" data are the cooling data taken on the first cooling run for a sample that has never been cooled below the polymerization temperature.[8,9] We do not understand why equilibration for depolymerization is so much slower than equilibration for polymerization. That the scattering intensity for the nonequilibrated heating runs was greater than that for the equilibrated cooling runs suggests that the polymer molecules persisted in a metastable state at degrees of polymerization greater than those of the equilibrium state. The remarkable observation that a sample "annealed" well above the polymerization temperature *returned to the state of the initial cooling run* supports the hypothesis of metastable polymer molecules. Comparison between samples 91-3 and 92-1, which were prepared with the same concentration of initial monomer and of initiator, is very interesting. These two samples had very different thermal histories: sample 91-3 was cooled slowly, without any heating, while sample 92-1 was successively cooled and heated by small steps and with an overall slow cooling. The value of T_p and the general shape of $I(0,T)$ were the same for the two samples. The characteristic length, $\xi(T)$, rose to a larger value in 92-1, with the position of the peak, ξ^*, being the same. Perhaps the different behavior of $\xi(T)$ in samples 92-1 was due to an out-of-equilibrium distribution of polymers, caused by the heating steps. These observations indicate the importance of kinetic problems in these systems. We plan to study the intriguing kinetics of these processes further.

Acknowledgment. We thank J. P. Ambroise for his help with the thermostat and the spectrometer. This work was supported in France by the Centre National de la Recherche Scientifique. The work in the U.S. was supported by the National Science Foundation under Grants CHE-9301027, CHE-9001056, and INT-9016061.

References and Notes

(1) Szwarc, M. *Carbanions, Living Polymers, and Electron Transfer Processes*; John Wiley-Interscience: New York, 1968.
(2) Webster, O. W. *Science* **1991**, *251*, 887.
(3) Szwarc, M.; Van Beylen, M. *Ionic Polymerization and Living Polymers*; Chapman and Hall: New York, 1993.
(4) Tobolsky, A. V. *J. Polym. Sci.* **1957**, *25*, 220. Tobolsky, A. V.; Eisenberg, A. *J. Am. Chem. Soc.* **1960**, *82*, 289. Tobolsky, A. V.; Eisenberg, A. *J. Colloid Sci.* **1962**, *17*, 49.
(5) Scott, R. L. *J. Phys. Chem.* **1965**, *69*, 261.
(6) Wheeler, J. C.; Kennedy, S. J.; Pfeuty, P. *Phys. Rev. Lett.* **1980**, *45*, 1748. Wheeler, J. C.; Pfeuty, P. *Phys. Rev. A* **1981**, *24*, 1050.
(7) Kennedy, S. J.; Wheeler, J. C. *J. Chem. Phys.* **1983**, *78*, 953.
(8) Zheng, K. M.; Greer, S. C. *Macromolecules* **1992**, *25*, 6128.
(9) Zheng, K. M.; Greer, S. C.; Corrales, L. R.; Ruiz-Garcia, J. *J. Chem. Phys.* **1993**, *98*, 9873.
(10) Ruiz-Garcia, J.; Greer, S. C. *Phys. Rev. Lett.* **1990**, *64*, 1983, 3204.
(11) Ruiz-Garcia, J. Ph.D. Dissertation, The University of Maryland at College Park, College Park, MD, 1989.
(12) Zheng, K. M. Ph.D. Dissertation, The University of Maryland at College Park, College Park, MD, 1991.
(13) Ploplis Andrews, A. Ph.D. Dissertation, The University of Maryland at College Park, College Park, MD, 1993.
(14) Andrews, Kevin P. Ph.D. Dissertation, The University of Maryland at College Park, College Park, MD, 1994.
(15) Pfeuty, P.; Boué, F.; Ambroise, J. P.; Bellissent, R.; Zheng, K. M.; Greer, S. C. *Macromolecules* **1992**, *25*, 5539.
(16) Szwarc, M.; Levy, M.; Milkovich, R. *J. Am. Chem. Soc.* **1956**, *78*, 2656.
(17) Flory, P. J. *Principles of Polymer Chemistry*; Cornell University Press: Ithaca, NY, 1953.
(18) Barton, A. F. M., Ed. *CRC Handbook of Polymer–Liquid Interaction Parameters and Solubility Parameters*; CRC Press: Boca Raton, FL, 1990.
(19) Wheeler, J. C.; Pfeuty, P. M. *Phys. Rev. Lett.* **1993**, *71*, 1653.
(20) (a) Wheeler, J. C.; Pfeuty, P. *Phys. Rev. Lett.* **1981**, *16*, 1409. (b) Wheeler, J. C.; Pfeuty, P. *J. Chem. Phys.* **1981**, *74*, 6415.
(21) de Gennes, P.-G. *Phys. Lett.* **1972**, *38*, 339.
(22) des Cloizeaux, J. *J. Phys. (Orsay, Fr.)* **1975**, *36*, 281.
(23) Wheeler, J. C.; Pfeuty, P. *J. Chem. Phys.* **1981**, *74*, 6415.
(24) Furman, D.; Blume, M. *Phys. Rev. B* **1974**, *10*, 2068.
(25) Edwards, S. F. *Proc. Phys. Soc. (London)* **1966**, *88*, 265.
(26) Joyce, G. S. In *Phase Transitions and Critical Phenomena*; Domb, C., Green, M. S., Eds.; Academic Press: New York, 1972; Vol. 2.
(27) Joyce, G. S. *Philos. Trans. R. Soc. London* **1973**, *A273*, 583.
(28) Joyce, G. S. *J. Math. Phys.* **1971**, *12*, 1390.
(29) There is a sign error in the expression for eq 7 in ref 13.
(30) Boué, F.; Ambroise, J. P.; Bellissent, R.; Pfeuty, P. *J. Phys. I Fr.* **1992**, *2*, 969.
(31) Binney, J. E.; Dowrick, N. J.; Fisher, A. J.; Newman, M. E. J. *The Theory of Critical Phenomena: An Introduction to the Renormalization Group*; Oxford: New York, 1992.
(32) Le Guillou, J. C. *J. Phys. Lett.* **1985**, *46*, L-137.
(33) Peebles, L. *Molecular Weight Distributions in Polymers*; Interscience Publishers: New York, 1971.
(34) Das, S. Sarkar; Ploplis Andrews, A.; Greer, S. C., work in progress.
(35) Fujita, H. *Polymer Solutions*; Elsevier: New York, 1990.
(36) de Gennes, P.-G. *Scaling Concepts in Polymer Physics*; Cornell University Press: Ithaca, NY, 1979; p 40.
(37) Ballard, D. G.; Rayner, M. J.; Schelten, J. *Polymer* **1976**, *17*, 349.
(38) Feigin, L.; Svergun, D. I. *Structure Analysis by Small-Angle X-ray and Neutron Scattering*; Plenum Press: New York, 1987.
(39) Daoud, M.; Cotton, J. P.; Farnoux, B.; Jannick, G.; Sarma, G.; Benoit, H.; Duplessix, R.; Picot, C.; de Gennes, P.-G. *Macromolecules* **1975**, *8*, 804.
(40) Oberthur, R. C., private communication.
(41) Damay, P.; Leclerq, F.; Chieux, P. *Phys. Rev. B* **1989**, *40*, 4696. Bhatia, A. B.; Thornton, D. E. *Phys. Rev. B* **1970**, *2*, 3004.
(42) Stanley, H. E. *Introduction to Phase Transitions and Critical Phenomena*; Oxford University Press: New York, 1971.
(43) Damay, P.; Leclerq, F.; Chieux, P. *Physica B* **1989**, *156*, 223.
(44) See, for example: Dudowicz, J.; Lifschitz, M.; Freed, K. F.; Douglas, J. F. *J. Chem. Phys.* **1993**, *99*, 4804. Janssen, S.; Schwahn, D.; Speinger, T. *Phys. Rev. Lett.* **1992**, *68*, 3180.
(45) MATLAB, The MathWorks, Inc.: Natick, MA, 1992.
(46) Deming, S. N.; Morgan, S. L. *Anal. Chem.* **1973**, *45*, 278A.
(47) Roberts, D. E.; Jessup, R. W. *J. Res. Natl. Bur. Stand.* **1951**, *46*, 11.
(48) Press, W. H.; Flannery, B. P.; Teukolsky, S. A.; Vetterling, W. T. *Numerical Recipes: The Art of Scientific Computing*; Cambridge University Press: New York, 1986.
(49) des Cloizeaux, J.; Jannink, G. *Polymers in Solution: Their Modelling and Structure*; Clarendon Press: Oxford, 1990.
(50) Wiltzius, P.; Haller, H. R.; Cannell, D. S.; Schaefer, D. W. *Phys. Rev. Lett.* **1983**, *51*, 1183.
(51) Reference 36, p 299ff.